

# Energy Shaping for Stably Coordinating Internally Actuated Underwater Vehicles

WU Fan, GENG Zhiyong

The State Key Laboratory for Turbulence and Complex Systems, College of Engineering,  
Peking University, Beijing 100871, P. R. China  
E-mail: wufan@pku.edu.cn

**Abstract:** This paper considers the problem of stabilization and coordination for underwater vehicles using internal moving mass actuators. The underwater vehicle (UV) is modeled as a neutrally buoyant, bottom-heavy, submerged rigid body in an ideal fluid. The force of interaction between the UV and internal moving mass destabilizes UV's steady translation along its long axis if the moving mass is allowed to move freely inside the UV body. However, this interaction force can also be treated as a control input. Energy shaping is applied to control the motion of moving mass relative to the UV body such that the UV's steady long axis translation with a designated attitude is stabilized. The proposed method is extended to design control laws to coordinate steady motions of multiple UVs.

**Key Words:** Moving Mass Actuator, Energy Shaping, Stabilization, Coordination

## 1 Introduction

Internally actuated systems are enjoying more and more attention from space and ocean engineers as well as control theorists. In space applications, internal actuators are useful because they can be powered using readily generated electricity rather than costly propellant [1]. Internal moving mass actuators have been proposed as a cost-effective means for precision orbit control in spacecraft formations [2]. Internal actuators have also been used for a hypersonic re-entry vehicle, because the temperature and pressure outside are very high for conventional external control devices [3]. In ocean applications, internal actuators are appealing because they can be used at low velocity, where fins lose control authority [4]. Besides, internal actuators are not susceptible to corrosion and biological fouling. A fleet of underwater gliders equipped with internal buoyancy engines and mass redistribution systems are used to form mobile sensor networks to provide ocean sampling data over long time periods [5]. On the theoretical side, internally actuated systems are often underactuated thus are difficult to control, they provide a rich test bed for newly developed control techniques.

Mechanical systems with internal moving mass actuators form an important class of internally actuated systems. The behavior of a mechanical system is closely related to its energy. Moving mass actuators influence the system's behavior by changing the system's kinetic metric and potential energy. The controlled system remains mechanical, of which many structure properties can be exploited to help the stability analysis and control design. Mechanical systems with only internal actuators are necessarily not linearly controllable nor feedback linearizable since the total momentum is conserved. For the above consideration, energy based methods are promising for controlling internally actuated mechanical systems. First, the energy based method preserves the system's mechanical structure and does not rely on technical-driven techniques, like nonlinearity domination by feedback linearization or high gain. Second, the energy based method exploits conserved quantities of the system to construct Lyapunov functions explicitly.

Assisted by Lyapunov functions, the method obtains stability and control results that hold over a larger domain than can be obtained using linear analysis and design.

The energy based method used in this paper is energy shaping. The idea is to shape the potential and/or kinetic energy of the system in order to make the desired behavior a stable solution of the "shaped" system. Control forces and torques implement the difference between the shaped energy and the original energy. [6] initiates the energy shaping for stabilizing middle axis rotations of a rigid spacecraft using a single internal rotor. [4] employs kinetic energy shaping to stabilize steady motions of a UV using internal rotors. [7] uses the method of controlled lagrangians, an algorithmic energy shaping approach in the Lagrangian framework, to stabilize steady motions of vehicle systems with internal moving mass actuators. Without external control, a stable steady motion, i.e. relative equilibrium, is the best one can obtain. However, stable relative equilibria are important low-energy and natural motions of mechanical systems and provide attractive solutions to motion planning problems [8].

This paper studies the stabilization of a neutrally buoyant, bottom-heavy UV and coordination of multiple UVs for dynamics restricted to the vertical plane. The control is necessary because the coupling between UV and moving mass induces unstable dynamics. Potential shaping is performed to stabilize UV's relative equilibria, which correspond to steady long axis translations. Specifically, the original potential is shaped by adding a linear spring linking the moving mass and UV. Sufficient conditions on the spring stiffness are given to ensure that the total energy after shaping has an extremum at the desired relative equilibria. Asymptotic stability is obtained by feedback damping injection. The method is extended to design control laws to coordinate steady motions of multiple UVs. As far as authors know, the only work solving the stabilization and coordination problem for a class of underactuated mechanical systems using energy shaping is [9], wherein the underactuated control is applied externally. Based on feedback linearization, [10] uses only internal actuators to stabilize and coordinate underwa-

This work is supported by National Natural Science Foundation (NNSF) of China under Grant 11072002, 10832006.

ter gliders. However, external forces like gravity, buoyancy, lift, and drag assist in the control design. Unlike [10], this paper gives a nonlinear stability proof for relative equilibria in terms of energy, whereas in [10], the stability is proved only for the linearized model.

The paper is organized as follows. Section 2 describes the UV model. Section 3 derives the stabilizing control law based on potential shaping. Section 4 extends the control design to coordinate multiple UVs. Section 5 gives a numerical simulation to demonstrate the control results. Section 6 concludes the paper and gives future research problems.

## 2 UV Model

Fig. 1 depicts a UV, modeled as an ellipsoid with one moving mass constrained to move along a linear track fixed with respect to the UV body. Assume that the track is along the longest ellipsoid axis. The dynamic modeling procedure in [1] is used to derive equations of motion for the UV.

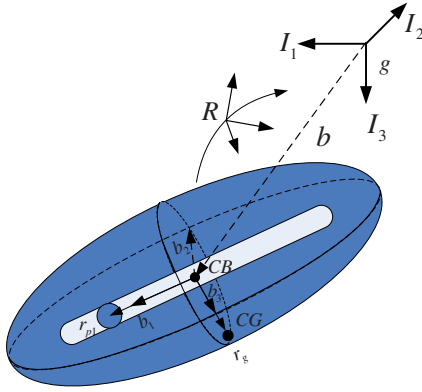


Fig. 1: Single UV with one moving mass along a track

A reference frame with orthonormal basis  $(\mathbf{I}_1, \mathbf{I}_2, \mathbf{I}_3)$  is fixed in the inertial space. Another reference frame with orthonormal basis  $(\mathbf{b}_1, \mathbf{b}_2, \mathbf{b}_3)$  is fixed in the UV body with its origin at the center of buoyancy (CB) and its axes aligned with the principal axes of the ellipsoid. The rotation matrix  $\mathbf{R} \in SO(3)$  transforms vectors from the body frame to the inertial frame. The vector  $\mathbf{b} \in \mathbb{R}^3$  locates the origin of the body frame in the inertial frame. Let  $\boldsymbol{\omega} \in \mathbb{R}^3$  and  $\mathbf{v} \in \mathbb{R}^3$  represent the angular and linear velocity of the UV with respect to the inertial frame respectively, both expressed in the body frame. Define the operator  $\hat{\cdot}$  by requiring that  $\hat{\mathbf{x}}\mathbf{y} = \mathbf{x} \times \mathbf{y}$  for all  $\mathbf{x}, \mathbf{y} \in \mathbb{R}^3$ . Let  $\mathbf{r}_p = r_{p1}\mathbf{b}_1$  be the position of the moving mass with respect to CB, and  $\mathbf{v}_p \in \mathbb{R}^3$  be the absolute velocity of the moving mass with respect to the inertial frame, both expressed in the body frame. The kinematics of the UV/moving mass system are given by

$$\begin{aligned} \dot{\mathbf{R}} &= \mathbf{R}\hat{\boldsymbol{\omega}}, \\ \dot{\mathbf{b}} &= \mathbf{R}\mathbf{v}, \\ \dot{\mathbf{r}}_p &= \mathbf{v}_p - \mathbf{v} - \boldsymbol{\omega} \times \mathbf{r}_p. \end{aligned} \quad (1)$$

Buoyancy and gravity play important roles in the UV dynamics. A buoyant force  $-mg\mathbf{I}_3$  acts on the UV body at CB, where  $m$  is the mass of the displaced fluid, and  $g$  is the acceleration of gravity. A gravitational force  $m_bg\mathbf{I}_3$  acts on the UV body at its center of gravity (CG), where  $m_b$  is the

mass of the UV body. The CG location is expressed in the body frame by  $\mathbf{r}_g = \gamma\mathbf{b}_3$ , where  $\gamma > 0$  means that the UV is bottom heavy. A gravitational force  $m_pg\mathbf{I}_3$  acts on the moving mass, where  $m_p$  is the mass of moving mass. Here and throughout, it is assumed that the UV/moving mass system is neutrally buoyant, that is,

$$m = m_b + m_p.$$

Because the UV is immersed in an infinite volume of ideal fluid that is at rest at infinity, the UV's motion induces motion in the surrounding fluid (and vice versa). The effect is captured by the added mass and added inertial, which account for the additional energy that is necessary to accelerate the fluid around the UV as it moves [4]. It will be assumed that the principal axes of the displaced fluid are the same as the principal axes of the UV body, such that the UV/fluid inertial and mass matrices  $\mathbf{J}_{b/f}$  and  $\mathbf{M}_{b/f}$  are diagonal. Let  $\boldsymbol{\psi} = (\boldsymbol{\omega}, \mathbf{v}, \dot{\mathbf{r}}_p)$  represent the generalized velocity, the Hamiltonian of UV/fluid/moving mass system is the sum of the kinetic energy and potential energy

$$H = \frac{1}{2}\boldsymbol{\psi}^T \mathbf{M} \boldsymbol{\psi} - (m_bg\mathbf{r}_g + m_pg\mathbf{r}_p) \cdot \boldsymbol{\Gamma}, \quad (2)$$

where  $\boldsymbol{\Gamma} = \mathbf{R}^T \mathbf{I}_3$  is the direction of gravity expressed in the body frame, and the matrix components of the kinetic energy metric are

$$\mathbf{M} = \begin{pmatrix} \mathbf{J}_{b/f} - m_p\hat{\mathbf{r}}_p\hat{\mathbf{r}}_p & m_b\hat{\mathbf{r}}_g + m_p\hat{\mathbf{r}}_p & m_p\hat{\mathbf{r}}_p \\ -m_b\hat{\mathbf{r}}_g - m_p\hat{\mathbf{r}}_p & \mathbf{M}_{b/f} + m_p\mathcal{I}_3 & m_p\mathcal{I}_3 \\ -m_p\hat{\mathbf{r}}_p & m_p\mathcal{I}_3 & m_p\mathcal{I}_3 \end{pmatrix},$$

where  $\mathcal{I}_3$  represents the  $3 \times 3$  identity matrix.

Let  $\mathbf{p}$  represent the linear momentum of the UV/fluid/moving mass system with respect to the inertial frame, expressed in the body frame. Let  $\boldsymbol{\pi}$  represent the angular momentum of the UV/fluid/moving mass system about the origin of the body frame. Let  $\mathbf{p}_p$  represent the linear momentum of the moving mass with respect to the inertial frame, expressed in the body frame. They are related to the general velocity  $\boldsymbol{\psi}$  through

$$\begin{pmatrix} \boldsymbol{\pi} \\ \mathbf{p} \\ \mathbf{p}_p \end{pmatrix} = \frac{\partial H}{\partial \boldsymbol{\psi}} = \mathbf{M} \begin{pmatrix} \boldsymbol{\omega} \\ \mathbf{v} \\ \dot{\mathbf{r}}_p \end{pmatrix}.$$

Hamiltonian (2) is invariant under arbitrary translations of the inertial frame and arbitrary rotations of the inertial frame about the direction of gravity, thus possesses symmetry with respect to UV's inertial position as well as rotation about the gravity direction. Through symmetry reduction, the reduced dynamics expressed in the body frame can be described by equations [1]

$$\begin{pmatrix} \dot{\boldsymbol{\pi}} \\ \dot{\mathbf{p}} \\ \dot{\mathbf{p}}_p \end{pmatrix} = \begin{pmatrix} \boldsymbol{\pi} \times \boldsymbol{\omega} + \mathbf{p} \times \mathbf{v} + \mathbf{X}_g \times \boldsymbol{\Gamma} \\ \mathbf{p} \times \boldsymbol{\omega} \\ \boldsymbol{\Gamma} \times \boldsymbol{\omega} \\ \mathbf{p}_p \times \boldsymbol{\omega} + m_pg\boldsymbol{\Gamma} \end{pmatrix} + \mathbf{u}, \quad (3)$$

where  $\mathbf{X}_g = (m_bg\mathbf{r}_g + m_pg\mathbf{r}_p)$ , and  $\mathbf{u}$  represents the control force acting on the moving mass along the  $\mathbf{b}_1$  axis by the UV body.



The potential shaping control law is

$$u = -\text{grad}V = -k_s r_{p1}, \quad (9)$$

where  $\text{grad}V$  denotes the gradient of  $V$ . The closed loop system is a mechanical system with a shaped Hamiltonian

$$H_V = H + V,$$

and possesses the same relative equilibrium as (7). One may find conditions for nonlinear stability using the energy-Casimir method [11]. This involves constructing a function  $H_\Phi = H_V + \Phi(C_1, C_2, C_3)$ , which has a strict minimum or maximum at the equilibrium. The function  $H_\Phi$  is conserved by construction, thus is automatically a Lyapunov function. Let

$$m_x = m_1 + m_p, \quad m_z = m_3 + m_p, \quad p_{e1} = m_x v_{e1}.$$

Notice that  $m_x < m_z$ .

**Proposition 1** Relative equilibrium (7) is stable if

$$\begin{aligned} J_2 &> \frac{\gamma^2 m_b^2}{m_x} \\ m_b g \gamma &> \left( \frac{1}{m_1} - \frac{1}{m_3} \right) p_{e1}^2 \\ k_s &> \frac{m_p^2 g^2 (m_x - m_z + m_x m_z)}{m_b g \gamma (m_x - m_z + m_x m_z) + (m_x - m_z) p_{e1}^2} \end{aligned} \quad (10)$$

Asymptotical stability is obtained by adding feedback dissipation

$$u = -k_s r_{p1} - k_{sd} \dot{r}_{p1}, \quad k_{sd} > 0. \quad (11)$$

*Proof.* A Lyapunov function for relative equilibrium (7), obtained by the energy-Casimir method, is

$$H_\Phi = H_V - \frac{C_1}{m_x} + \frac{1}{2} C_2^2 + \frac{1}{2} \left( C_1 - \frac{p_{e1}^2}{2} \right)^2.$$

Along equations of motion (6), one can check that  $\text{grad}H_\Phi = 0$ , and the Hessian  $\text{Hess}H_\Phi > 0$  when evaluated at relative equilibrium (7), provided that conditions (10) are satisfied. Nonlinear stability follows from Lyapunov direct method. Asymptotical stability follows from LaSalle invariance principle.

Spectral analysis shows that sufficient conditions (10) are sharp in the sense that relative equilibrium (7) is unstable if any one of the inequalities is reversed. The second inequality in (10) is the same as the stability result in [12], where it is shown that if a bottom heavy UV translates along its intermediate axis, and the vertical  $b_3$  axis is the minor axis, then CG should be sufficiently far below CB to ensure the steady motion stability.

Physically speaking, control law (16) works as linking the moving mass and the UV body with a linear damped spring. Since the bottom heaviness  $\gamma$  has already provided a restoring torque in pitch, the steady long axis translation can be stabilized by a sufficiently stiff spring to prevent large oscillations of the moving mass. This steady motion becomes unstable if the spring is too weak or the gliding speed is too fast.

Now, consider a two-parameter family of relative equilibrium denoted as

$$\begin{aligned} \theta &= \theta_e, \quad \omega_2 = 0, \quad v_1 = v_{e1}, \quad v_3 = 0, \\ r_{p1} &= -\frac{\gamma m_b \tan \theta_e}{m_p}, \quad \dot{r}_{p1} = 0, \quad u_e = m_p g \sin \theta_e. \end{aligned} \quad (12)$$

which corresponds to the UV's translation along the long axis with a constant pitch angle  $\theta_e$ .

Shaping potential (8) with  $k_s$  taking the value

$$k_{se} = \frac{g m_p^2 \cos \theta_e}{\gamma m_b} \quad (13)$$

makes (12) a relative equilibrium of the closed loop. However, simulation results show that only for large values of  $\theta_e$ , e.g.  $|\theta_e| > \pi/5$ , relative equilibrium (12) is stable. And for small values of  $\theta_e$ , (12) may become unstable. A possible explanation for this behavior is that the requirement that spring stiffness should not be too weak to prevent large moving mass oscillations is contradictory to fixing  $k_s$  as in (13) for small pitch angles.

A modified version for shaping potential (8) is

$$\bar{V} = \frac{1}{2} k_{se} r_{p1}^2 + \frac{1}{2} k_s (r_{p1} - r_d)^2, \quad (14)$$

where

$$r_d = -\frac{\gamma m_b \tan \theta_e}{m_p}.$$

**Proposition 2** Relative equilibrium (12) is stable if

$$\begin{aligned} J_2 &> \frac{\gamma^2 m_b^2}{m_x} \\ m_b g \gamma &> \left( \frac{1}{m_1} - \frac{1}{m_3} \right) p_{e1}^2 \\ -\frac{1}{2} \pi &< \theta_e < \frac{1}{2} \pi \\ k_s &> -k_{se} \\ &+ \frac{m_p^2 g^2 (m_x - m_z + m_x m_z)}{m_b g \gamma (m_x - m_z + m_x m_z) + (m_x - m_z) p_{e1}^2} \end{aligned} \quad (15)$$

Asymptotical stability is obtained by feedback dissipation

$$u = -k_{se} r_{p1} - k_s (r_{p1} - r_d) - k_{sd} \dot{r}_{p1}. \quad (16)$$

*Proof.* A Lyapunov function for relative equilibrium (12) is

$$\bar{H}_\Phi = H_{\bar{V}} - \frac{C_1}{m_x} + \frac{1}{2} \left[ (C_2 - C_{2e})^2 + \left( C_1 - \frac{p_{e1}^2}{2} \right)^2 \right],$$

where  $H_{\bar{V}} = H + \bar{V}$ ,  $C_{2e} = -m_x v_{e1} \sin \theta_e$ . Similar to the proof of Proposition 1, nonlinear stability follows from Lyapunov direct method, and asymptotical stability can be assessed by LaSalle invariance principle.

#### 4 Coordination

Now, we extend the control framework and consider steady motions of a group of  $N$  identical UVs. Coordination here means that each UV translates along their long axis steadily, with aligned pitch angles and a common gliding speed.

Recall that the UV dynamics evolve on a surface of constant linear momentum. In order to implement a stable, coordinated, steady motion, we make the following assumptions.



**Assumption 1** Casimirs  $C_1, C_2$  of each UV have the same value which are determined by evaluating  $C_1, C_2$  at the desired coordinated motion.

**Assumption 2**  $N$  UVs communicate with communication links characterized by the edges of a fixed, connected, and undirected graph.

Under Assumption 1 and 2, multiple UVs can be coordinated by synchronizing their moving mass positions. Moving mass synchronization can be obtained by potential shaping across the UV group.

First, one UV is chosen arbitrarily to be the leader. Without loss of generality, it is assigned index 1. UV1's Hamiltonian is shaped by

$$V_1 = \frac{1}{2}k_{se}r_{p1,1}^2 + \frac{1}{2}k_s(r_{p1,1} - r_d)^2.$$

The  $i$ th UV's Hamiltonian, for  $i = 2, \dots, N$ , is shaped by

$$V_i = \frac{1}{2}k_{se}r_{p1,i}^2.$$

Second, introduce an artificial potential across the group as

$$V_C = \frac{1}{2}k_{p,i} \sum_i \sum_{j \rightsquigarrow i} (r_{p1,i} - r_{p1,j})^2, \quad (17)$$

where  $k_{p,i} > 0$ , and  $j \rightsquigarrow i$  denotes that the  $j$ th UV sends information to the  $i$ th UV. Under Assumption 2,  $V_C$  has 0 as the only minimum when all moving mass positions are synchronized.

The total Hamiltonian of the UV group after potential shaping becomes

$$\hat{H} = \sum_{i=1}^N H_i + V_1 + \sum_{i=2}^N V_i + V_C, \quad (18)$$

where  $H_i$  is the original Hamiltonian of the  $i$ th UV. The potential shaping control law is

$$\begin{aligned} u_1 &= -k_{se}r_{p1,1} - k_s(r_{p1,1} - r_d) - k_{sd}\dot{r}_{p1,1}, \\ u_i &= -k_{se}r_{p1,i} - \sum_{j \rightsquigarrow i} \left( k_{p,i}(r_{p1,i} - r_{p1,j}) \right) - k_{d,i}\dot{r}_{p1,i}, \\ i &= 2, \dots, N. \end{aligned} \quad (19)$$

Control (19) indicates that the leader is controlled to the desired steady motion autonomously, while the rest UVs are coordinated by virtually linking moving mass in pairs of UVs through damped linear springs.

**Proposition 3** Consider  $N$  identical UVs satisfying Assumption 1 and 2. Under control (19), each UV converges to relative equilibrium (12) with aligned pitch angles and a common gliding speed.

*Proof.* A Lyapunov function is

$$\hat{H}_\Phi = \hat{H} + N \left( -\frac{C_1}{m_x} + \frac{1}{2}(C_2 - C_{2e})^2 + \frac{1}{2} \left( C_1 - \frac{p_{e1}^2}{2} \right)^2 \right). \quad (20)$$

Lyapunov direct method can be used again to verify the asymptotical stability of the coordinated steady motion.

The above coordinating control design can be extended to a group of UVs communicating on a disconnected, undirected graph. Divide UVs into several subgroups such that the communication graph of each subgroup is connected. It remains to choose a leader for each subgroup, and apply the coordinating control. Coordinated steady motions can be obtained as long as Assumption 1 is satisfied.

## 5 Simulation Example

We illustrate the coordinating control with a numerical simulation. Consider a group of two identical UVs (UV1 and UV2) and assume that UV1 is the leader. The model parameters are given as follows

$$\begin{aligned} m_b &= 10\text{kg}, m_1 = 12\text{kg}, m_3 = 24\text{kg}, m_p = 2\text{kg}, \\ J_2 &= 0.1\text{Nm}^2, \gamma = 0.05\text{m}, g = 9.8\text{m/s}^2. \end{aligned}$$

**Case I.** The desired coordinated motion is that for  $i = 1, 2$

$$\begin{aligned} \theta_{ie} &= 0, \omega_{2,ie} = 0, v_{1,ie} = 0.5 \text{ m/s}, \\ v_{3,ie} &= 0, r_{p1,ie} = 0, \dot{r}_{p1,ie} = 0. \end{aligned}$$

According to (19), UV1 is applied the control

$$u_1 = -k_{se}r_{p1,1} - k_s r_{p1,1} - k_{sd}\dot{r}_{p1,1},$$

UV2 is applied the control

$$u_2 = -k_{se}r_{p1,2} - k_p(r_{p1,2} - r_{p1,1}) - k_d\dot{r}_{p1,2},$$

where  $k_{se}$  is computed as  $gm_p^2/(\gamma m_b)$ , and choose

$$k_s = 150, k_{sd} = 15, k_p = 150, k_d = 15.$$

One may verify that these choices satisfy the sufficient conditions in Proposition 2.

Assumption 1 requires that for  $i = 1, 2$

$$\mathbf{p}(0)_i \cdot \boldsymbol{\Gamma}_i(0) = 0, \quad \mathbf{p}(0)_i \cdot \mathbf{p}(0)_i = \mathbf{p}_{ie} \cdot \mathbf{p}_{ie}.$$

The latter equations are quadratic in  $v_{1,i}(0)$  and  $v_{3,i}(0)$ , there are at most two real values for each initial velocity given  $\mathbf{p}_{ie}$ ,  $\theta_{ie}$  and  $\theta_i(0)$ . Choose one set of initial conditions as

$$\begin{aligned} &(\theta_1, \omega_1, v_{1,1}, v_{3,1}, r_{p1,1}, \dot{r}_{p1,1})(0) \\ &= (-\pi/5, 0.01, 0.4042, -0.1585, -0.28, 0). \\ &(\theta_2, \omega_2, v_{1,2}, v_{3,2}, r_{p1,2}, \dot{r}_{p1,2})(0) \\ &= (-\pi/2.8, 0.01, 0.2166, -0.2425, 0.08, 0). \end{aligned}$$

Fig. 3 shows the simulation result achieving coordination.

Choose another set of initial conditions as

$$\begin{aligned} &(\theta_1, \omega_1, v_{1,1}, v_{3,1}, r_{p1,1}, \dot{r}_{p1,1})(0) \\ &= (-\pi/5, 0.01, -0.4042, 0.1585, -0.28, 0). \\ &(\theta_2, \omega_2, v_{1,2}, v_{3,2}, r_{p1,2}, \dot{r}_{p1,2})(0) \\ &= (-\pi/2.8, 0.01, -0.2166, 0.2425, 0.08, 0). \end{aligned}$$

Instead of coordination, each UV converges to another relative equilibrium corresponding to a steady translation along the opposite direction of  $\mathbf{b}_1$ -axis as shown in Fig. 4.

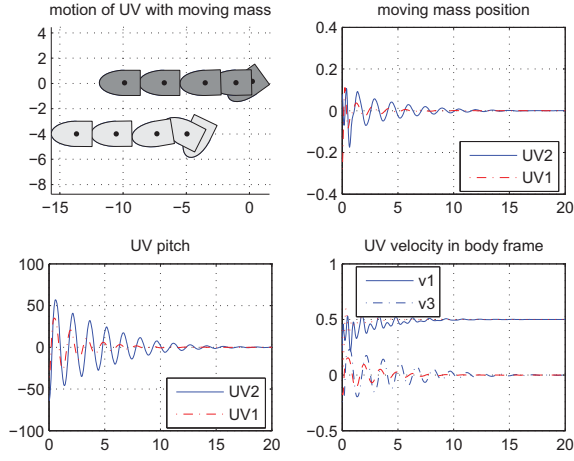


Fig. 3: Coordination with zero pitch angle

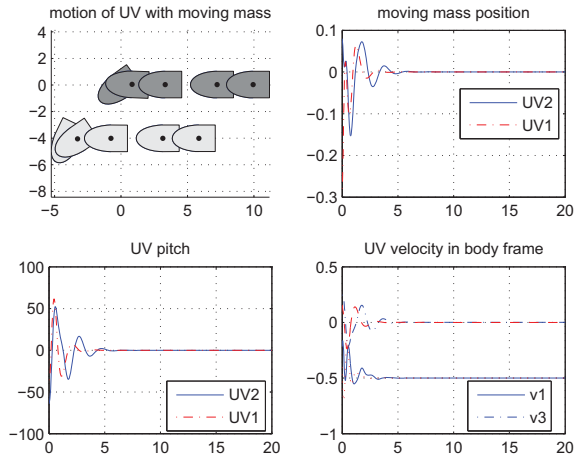


Fig. 4: Steady translation along the opposite  $b_1$ -axis

**Case II.** The desired coordinated motion is that for  $i = 1, 2$

$$\begin{aligned}\theta_{ie} &= (\pi/4) \text{ rad}, \omega_{2,ie} = 0, v_{1,ie} = 0.5 \text{ m/s}, \\ v_{3,ie} &= 0, r_{p1,ie} = r_d, \dot{r}_{p1,ie} = 0,\end{aligned}$$

where the equilibrium position of the moving mass is computed as

$$r_d = -\frac{\gamma m_b \tan(\pi/4)}{m_p}.$$

UV1 is applied the control

$$u_1 = -k_{se}r_{p1,1} - k_s(r_{p1,1} - r_d) - k_{sd}\dot{r}_{p1,1},$$

UV2 is applied the control

$$u_2 = -k_{se}r_{p1,2} - k_p(r_{p1,2} - r_{p1,1}) - k_d\dot{r}_{p1,2},$$

where  $k_{se}$  is computed as

$$k_{se} = \frac{gm_p^2 \cos(\pi/4)}{\gamma m_b}.$$

Choose the control parameters according to Proposition 2 as

$$k_s = 75, k_{sd} = 25, k_p = 75, k_d = 25.$$

Assumption 1 requires that for  $i = 1, 2$

$$\begin{aligned}\mathbf{p}_i(0) \cdot \boldsymbol{\Gamma}_i(0) &= \mathbf{p}_{ie} \cdot (-\sin \theta_{ie}, 0, \cos \theta_{ie}), \\ \mathbf{p}_i(0) \cdot \mathbf{p}_i(0) &= \mathbf{p}_{ie} \cdot \mathbf{p}_{ie}.\end{aligned}$$

Choose one set of initial conditions as

$$\begin{aligned}(\theta_1, \omega_1, v_{1,1}, v_{3,1}, r_{p1,1}, \dot{r}_{p1,1})(0) &= (-\pi/15, 0.01, 0.2719, -0.2258, -0.08, 0). \\ (\theta_2, \omega_2, v_{1,2}, v_{3,2}, r_{p1,2}, \dot{r}_{p1,2})(0) &= (-\pi/3, 0.01, -0.1298, -0.2600, 0.08, 0).\end{aligned}$$

Fig. 5 shows the simulation result achieving coordination.

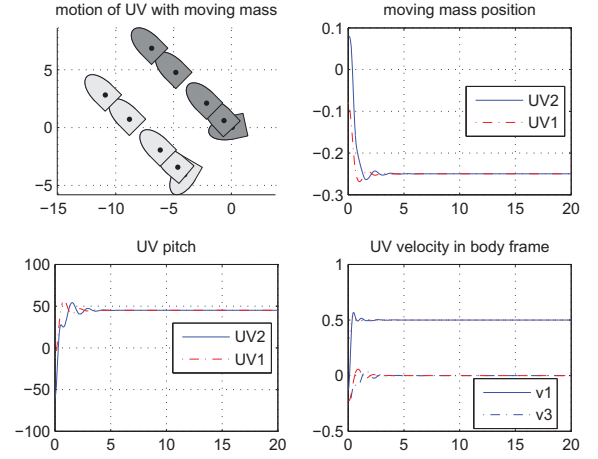


Fig. 5: Coordination with nonzero pitch angle

Choose another set of initial conditions as

$$\begin{aligned}(\theta_1, \omega_1, v_{1,1}, v_{3,1}, r_{p1,1}, \dot{r}_{p1,1})(0) &= (-\pi/15, 0.01, -0.4190, -0.1467, -0.08, 0). \\ (\theta_2, \omega_2, v_{1,2}, v_{3,2}, r_{p1,2}, \dot{r}_{p1,2})(0) &= (-\pi/3, 0.01, -0.4826, 0.069, 0.08, 0).\end{aligned}$$

Instead of coordination, each UV converges to another relative equilibrium corresponding to a steady translation along the opposite direction of  $b_3$ -axis as shown in Fig. 6.

The above simulation results illustrate that the region of attraction is limited by the proximity of the nearest neighboring relative equilibrium. Neighboring relative equilibria exist due to the translational symmetry. External forces and/or torques are needed to break the symmetry, thus exclude these relative equilibria.

## 6 Conclusions

In this paper, we have considered the problem of stabilization and coordination of UVs with internal moving mass actuators. The feedback control is designed in the context of mechanics, and does not rely on the linearization or cancellation of the nonlinearities. The proposed potential shaping laws have physical meaning, and can be easily implemented. Being energy based, the design method provides Lyapunov functions constructively, and gives nonlinear stability proofs for the relative equilibria.

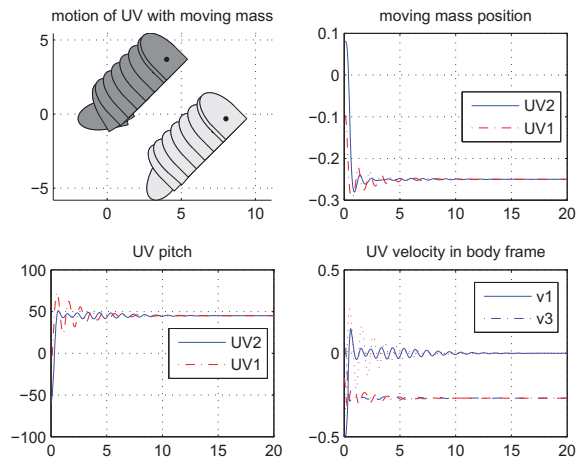


Fig. 6: Steady translation along the opposite  $b_3$ -axis

Without external forces or torques, both the stabilization and coordination are restricted to a constant momentum surface which makes the control problem academic. To combine the external control with internal actuation, and use energy shaping to solve the stable coordination problem is our ongoing work. It also needs to consider hydrodynamic forces when modeling the UV to make the control design more realistic to real engineering problems.

## References

- [1] C. A. Woolsey. Reduced Hamiltonian Dynamics for a Rigid Body Coupled to a Moving Mass Particle. *AIAA Journal of*

*Guidance, Control, and Dynamics*, 2005, 28(1): 131-138.

- [2] I. M. Ross. Mechanism for Precision Orbit Control with Applications to Formation Flying. *AIAA Journal of Guidance, Control, and Dynamics*, 2002, 25(4): 818-820.
- [3] R. D. Robinett III, B. R. Sturgis, S. A. Kerr. Moving-mass Roll Control System for Fixed-trim Re-entry Vehicle. *AIAA Journal of Guidance, Control, and Dynamics*, 1996, 19(5): 1064-1070.
- [4] C. A. Woolsey, N. E. Leonard. Stabilizing Underwater Vehicle Motion using Internal Rotors. *Automatica*, 2002, 38(2002): 2053-2062.
- [5] E. Fiorelli, N. E. Leonard, P. Bhatta, et al. Multi-AUV Control and Adaptive Sampling in Monterey Bay. *IEEE Journal of Oceanic Engineering*, 2006, 31(4): 935-948.
- [6] A. M. Bloch, P. S. Krishnaprasad, J. E. Marsden et al. Stabilization of Rigid Body Dynamics by Internal and External Torques. *Automatica*, 1992, 28(4): 745-756.
- [7] C. K. Reddy. Practical Challenges in the Method of Controlled Lagrangians. *PhD thesis*, Virginia Polytechnic Institute and State University, 2005.
- [8] P. Bhatta. Nonlinear Stability and Control of Gliding Vehicles. *PhD thesis*, Princeton University, 2006.
- [9] S. N. Nair, N. E. Leonard. Stable Synchronization of Mechanical System Networks. *SIAM Journal on Control and Optimization*. 2008, 47(2): 661-683.
- [10] P. Bhatta, N. E. Leonard. Stabilization and Coordination of Underwater Gliders. In *Proceedings of the 41st IEEE Conference on Decision and Control*, Las Vegas, Nevada, 2002, 2081-2086.
- [11] J. E. Marsden, T. S. Ratiu. *Introduction to Mechanics and Symmetry*. Berlin, Springer Press, 1999.
- [12] N. E. Leonard. Stability of a Bottom-heavy Underwater Vehicle. *Automatica*, 1997, 33(3): 331-346.